S-NPP, N-20, and N-21 VIIRS Reflective Solar Bands On-orbit Radiometric Calibration and Performance

VIIRS Characterization Support Team (VCST), NASA GSFC
(presented by Ning Lei)

May 1, 2023

Objectives

1. Radiometric calibration improvements since last STM (Feb. 2021)
2. RSB radiometric performance update
3. Future works

What happened since STM 2021

S-NPP

- Safe mode occurred in July 2022 led to F-factor trending change for many RSBs
- Developed TOA reflectance factor uncertainty algorithm
- Improved L1B pixel saturation detection

N-20

- Sliding window (in time) approach, using F(moon): same approach employed by S-NPP
- Improved L1B pixel saturation detection

N-21

- Launched on Nov. 10, 2022
- First mission RSB F-factor LUTs delivered with screen functions derived from calibration data collected on yaw maneuver orbits

VIIRS RSB calibration

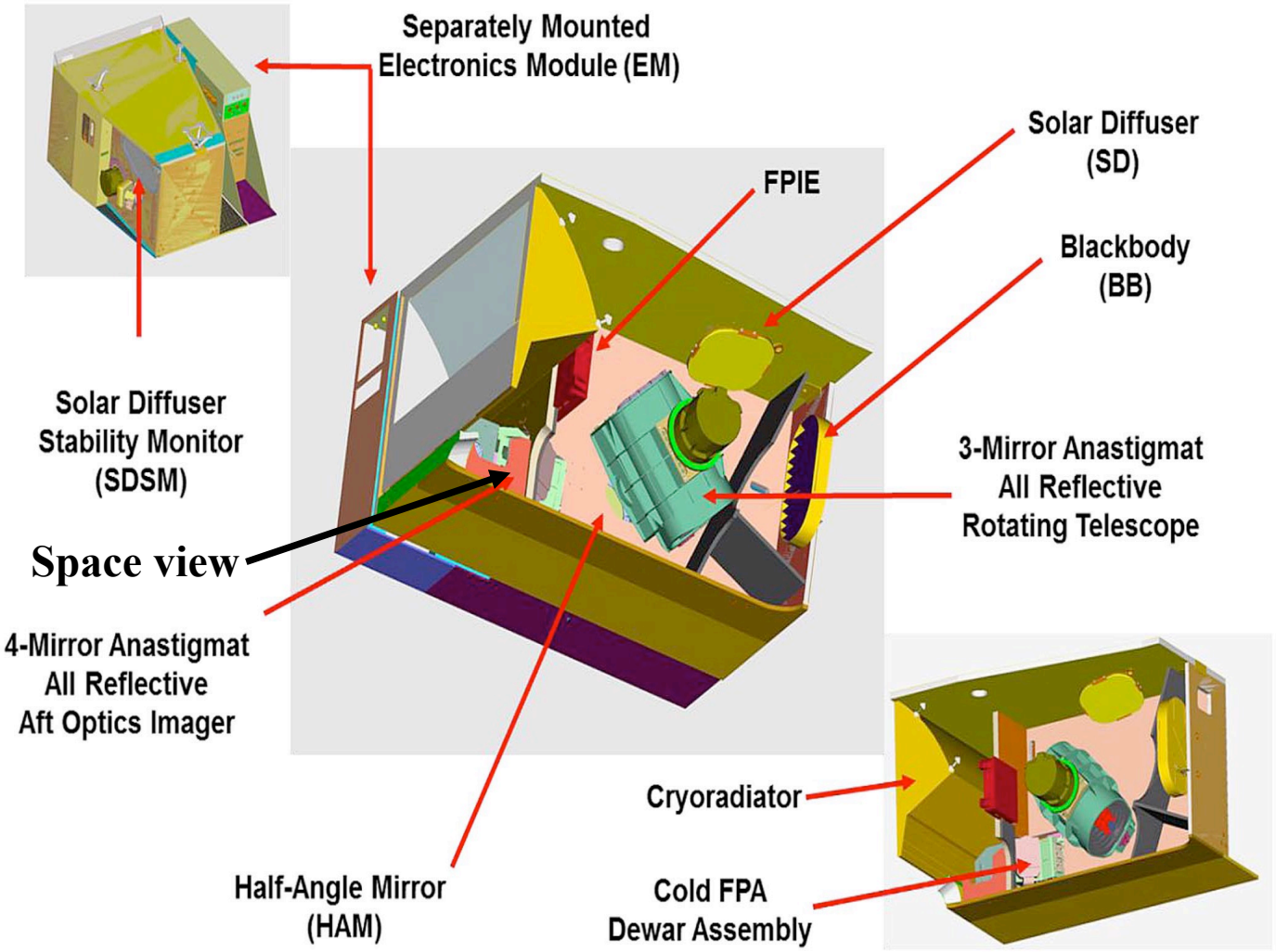

Spectral radiance

$$F(t,d)\sum_{i=0}^{3} c_i dn^i$$

$F(t,d)$ → **on-orbit calibrated**

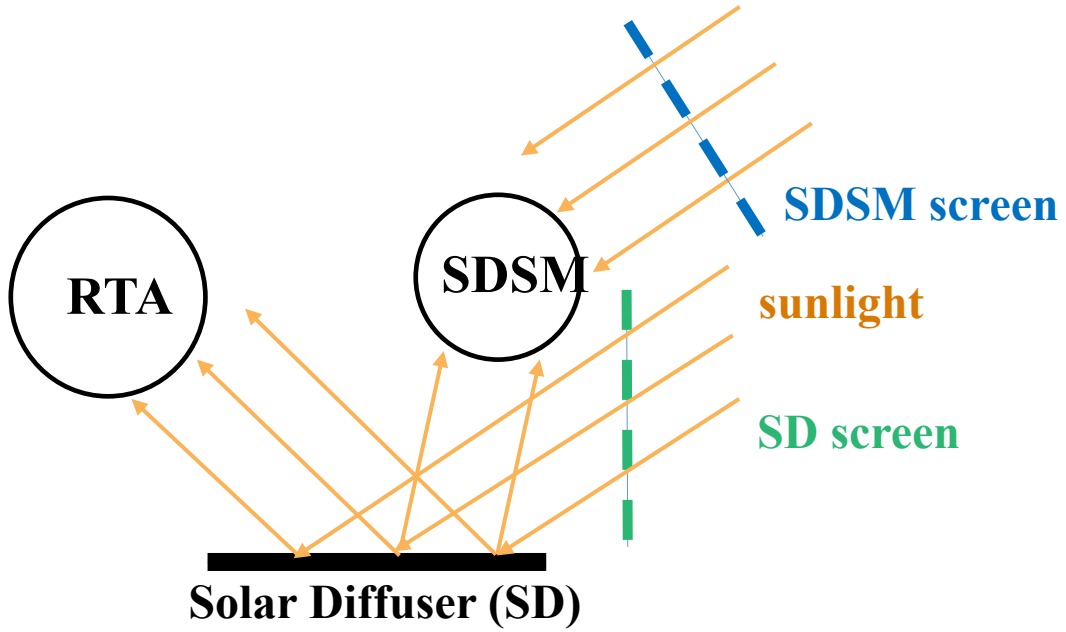

Solar Diffuser (SD): a calibration source; its BRDF change (H-factor) measured by the SD stability monitor (SDSM)

Performance of S-NPP SD and SDSM

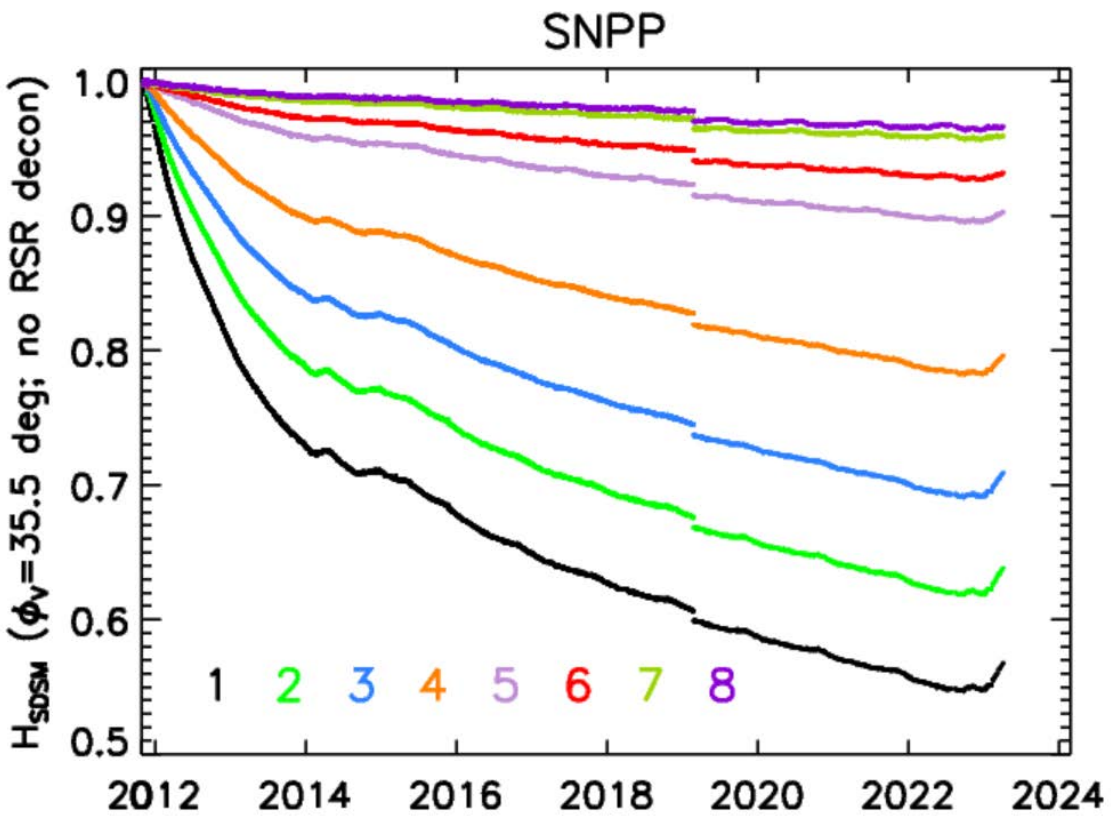

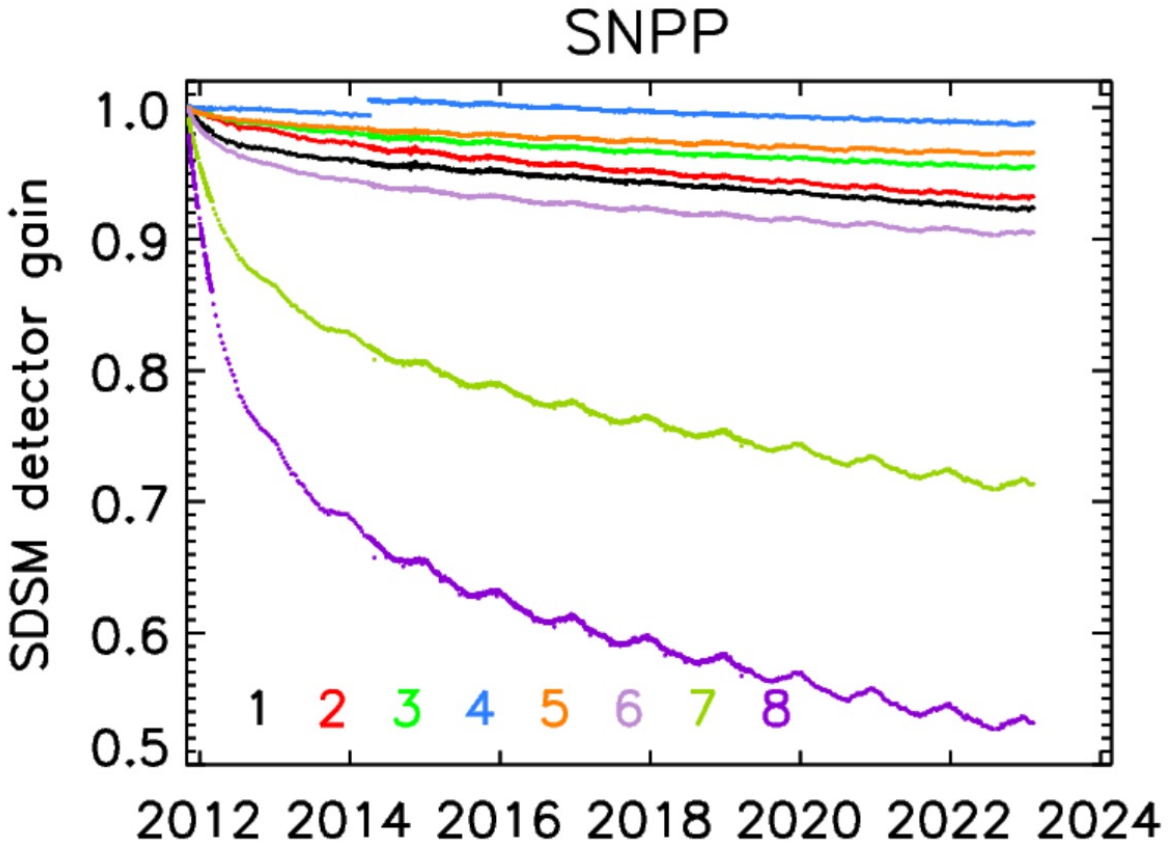

- SDSM detector gains trend normally
- H-factors dropped by about 1% due to the Feb. 24, 2019 event
- Recently, H-factors trend upwards (det 1-5), because of unusual solar activity impact on SD, also occurring for N20 and MODIS SDs

Calculate F(SD)

S-NPP and N-20

$$H_{\mathrm{RTA}} = H_{\mathrm{SDSM}} \times \frac{1 + \alpha_{\mathrm{RTA}}(\lambda) * (1 - H_{\mathrm{SDSM}})}{1 + \alpha_{\mathrm{H}}(\lambda) * (1 - H_{\mathrm{SDSM}}) * \left(\phi_{\mathrm{H,SD}}^{\mathrm{RTA}} - \phi_{\mathrm{H0}}\right)}$$

Solar azimuth angle

α_{RTA} and α_{H} obtained from fitting F(SD) to F(Moon)

Use a sliding window (in time) approach, fit F(H_{RTA}) to F(Moon) to find α_{RTA} *and* α_{H}

N-21

Not enough F(Moon) available to fit; choose to use the measured H_{SDSM} (no deconvolution)

S-NPP RSB 1/F-factors

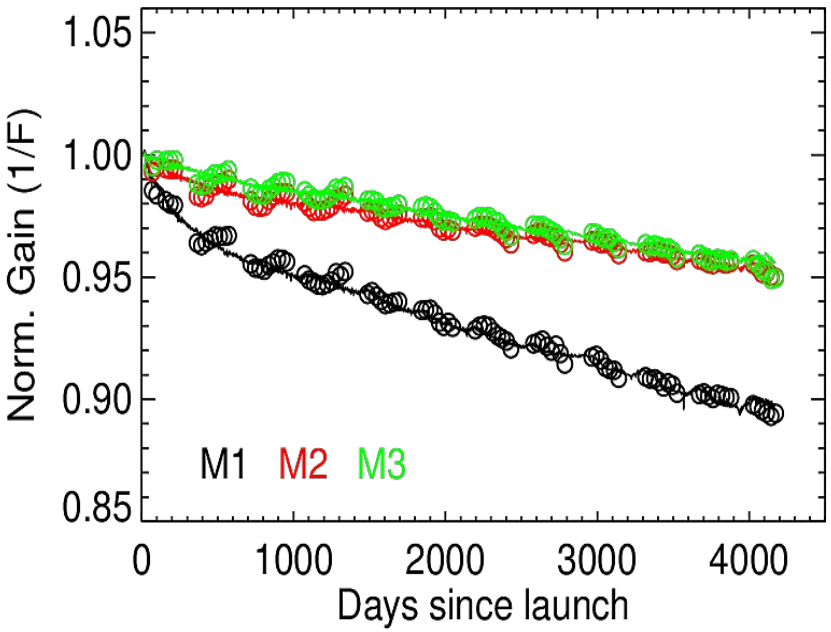

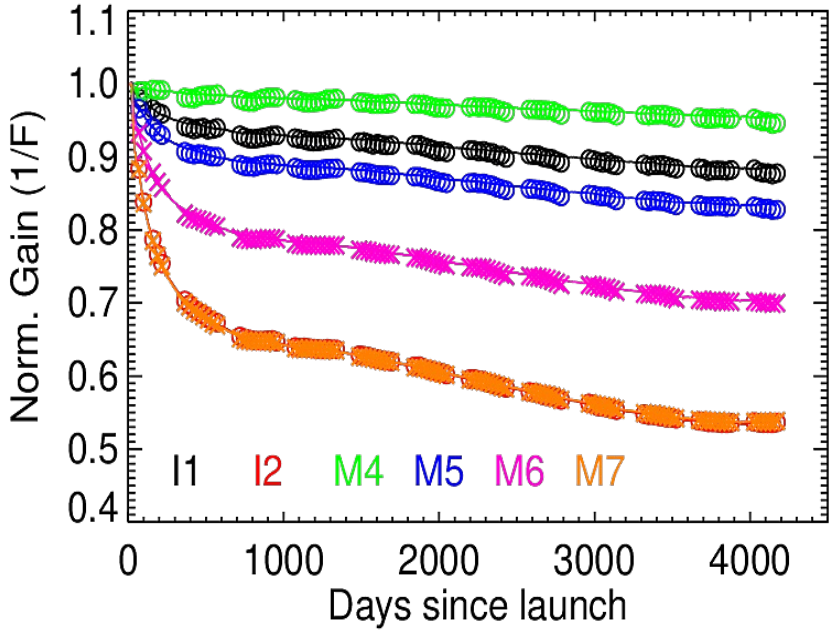

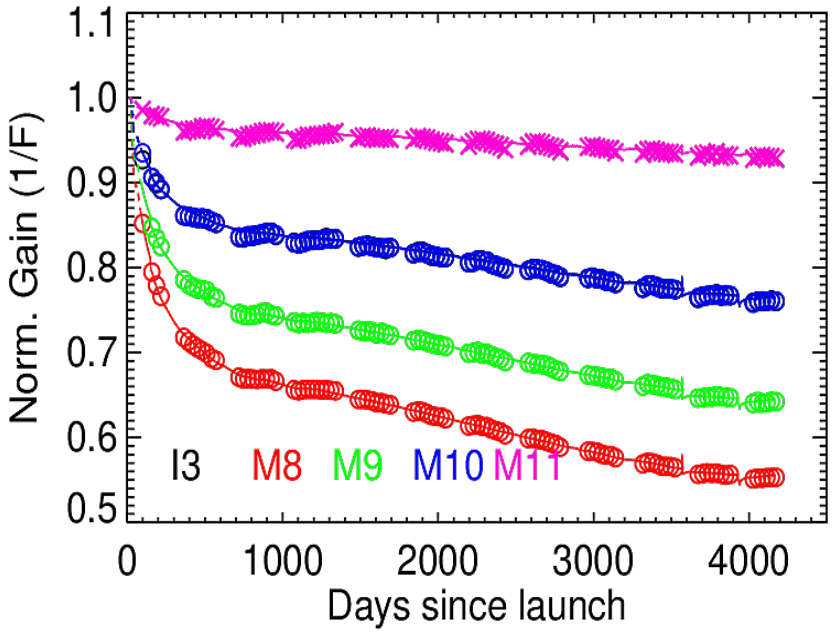

Solid lines: 1/F(SD); Circles: 1/F(Moon)

F decreases with time, because of telescope mirror surface tungsten oxide contamination

Performance of N-20 SD and SDSM

N-20 H-factors

$\phi_V = 35.5°$

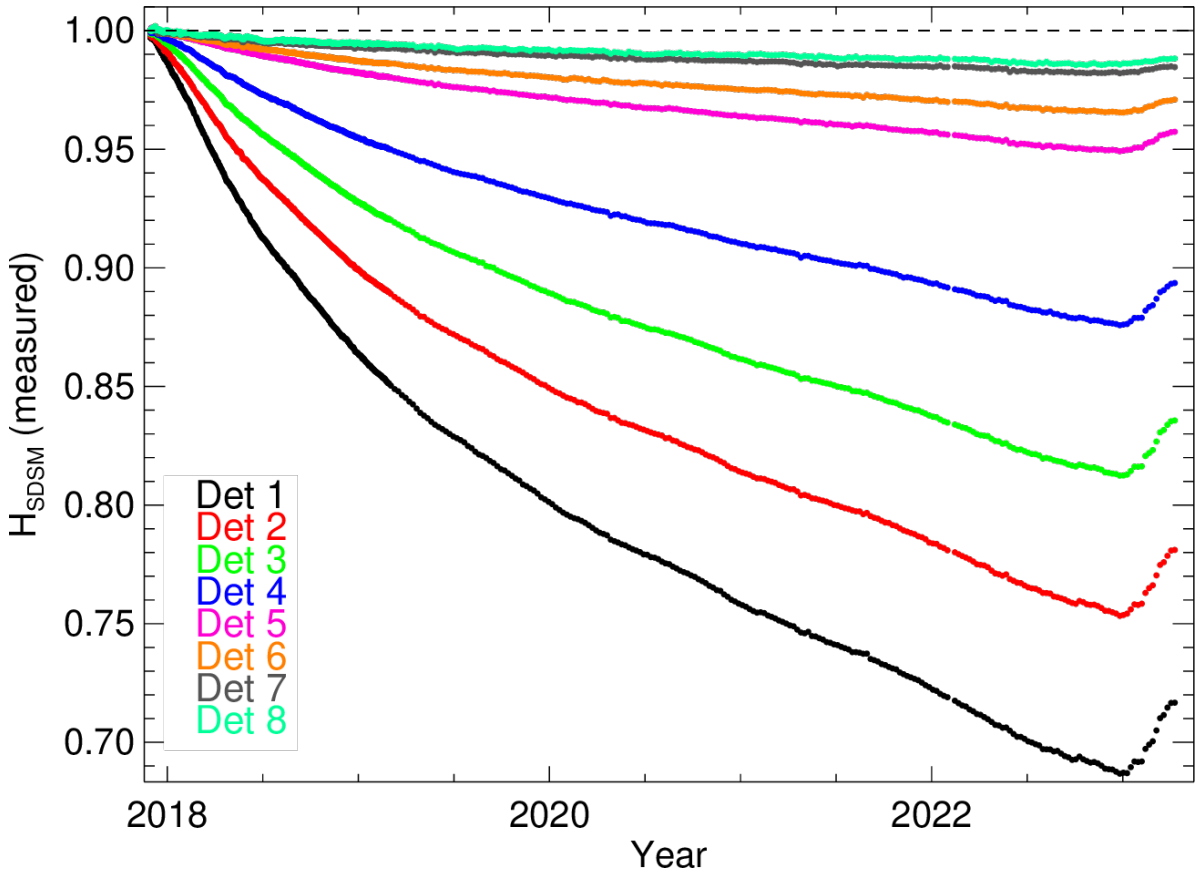

N-20 SDSM Detector Gains

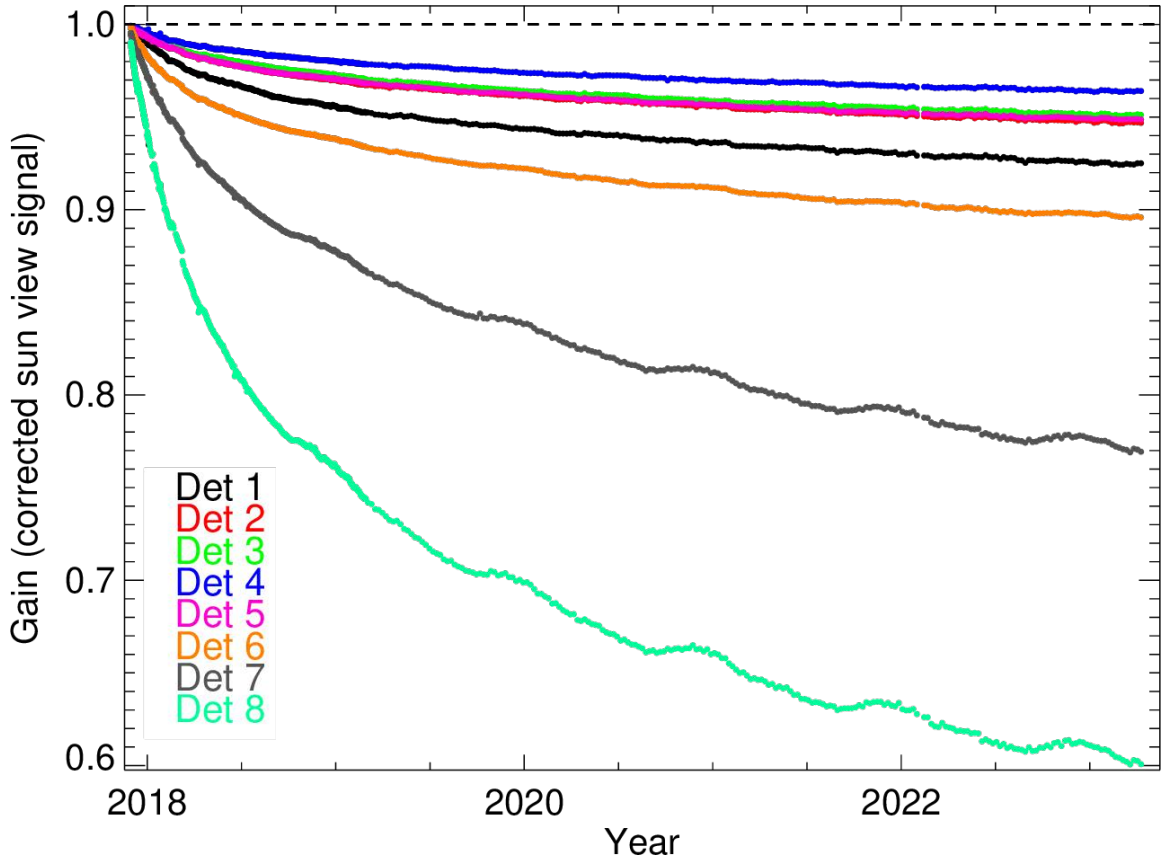

- **H-factors decrease at smaller rates than S-NPP H-factors**
- **SDSM gains decrease similarly to S-NPP**

N-20 RSB 1/F-factors

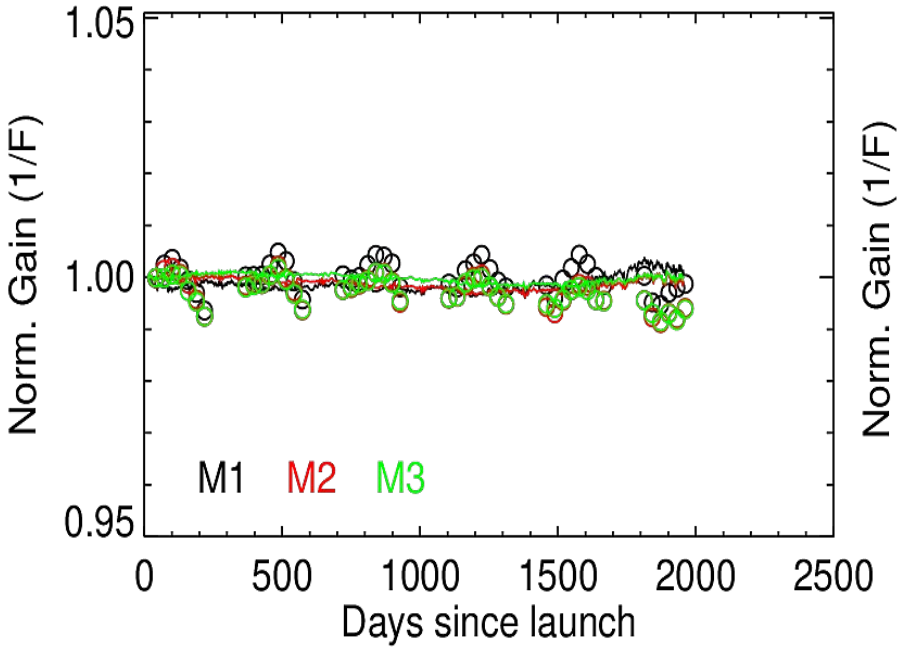

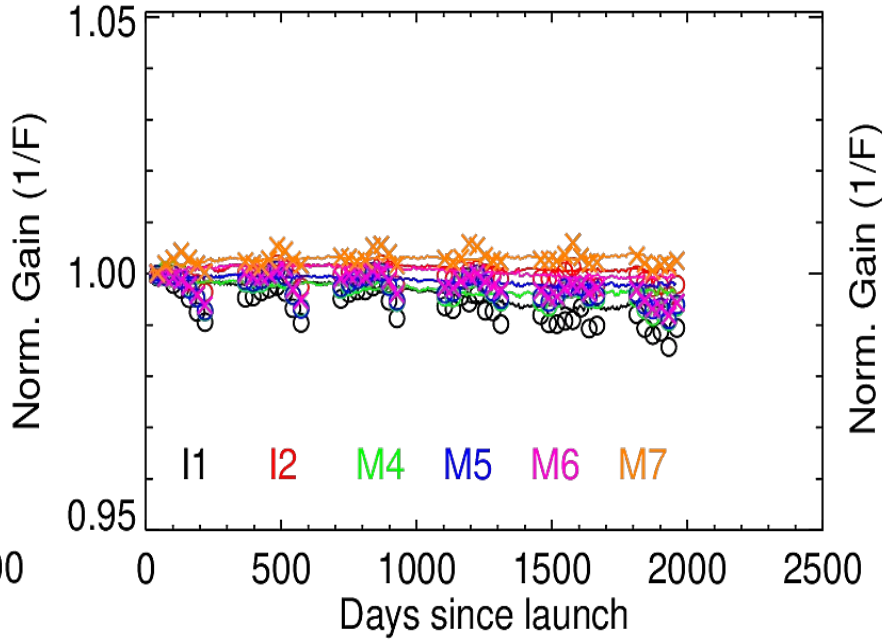

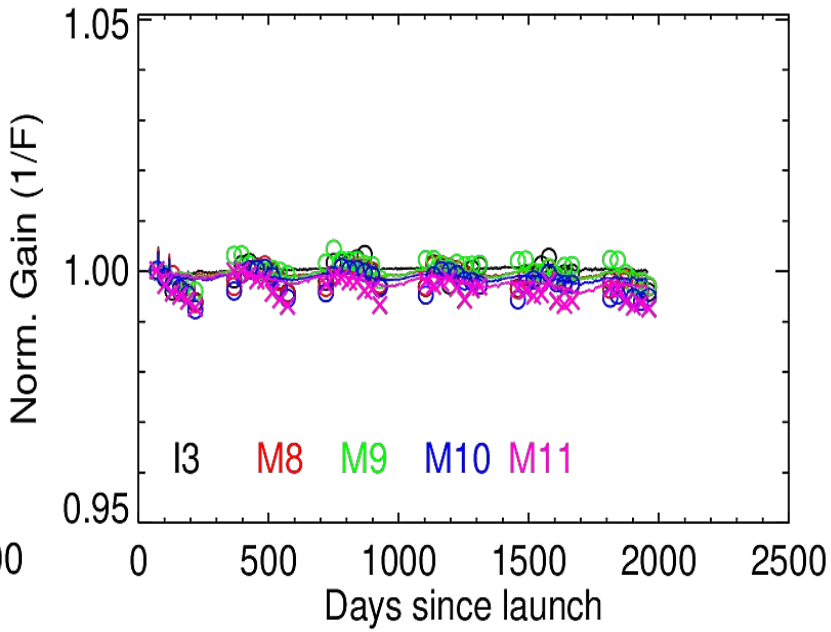

Solid lines: 1/F(SD); Circles: 1/F(Moon)

F-factors are very stable over mission

Performance of N-21 SD and SDSM

N-21 H-factors

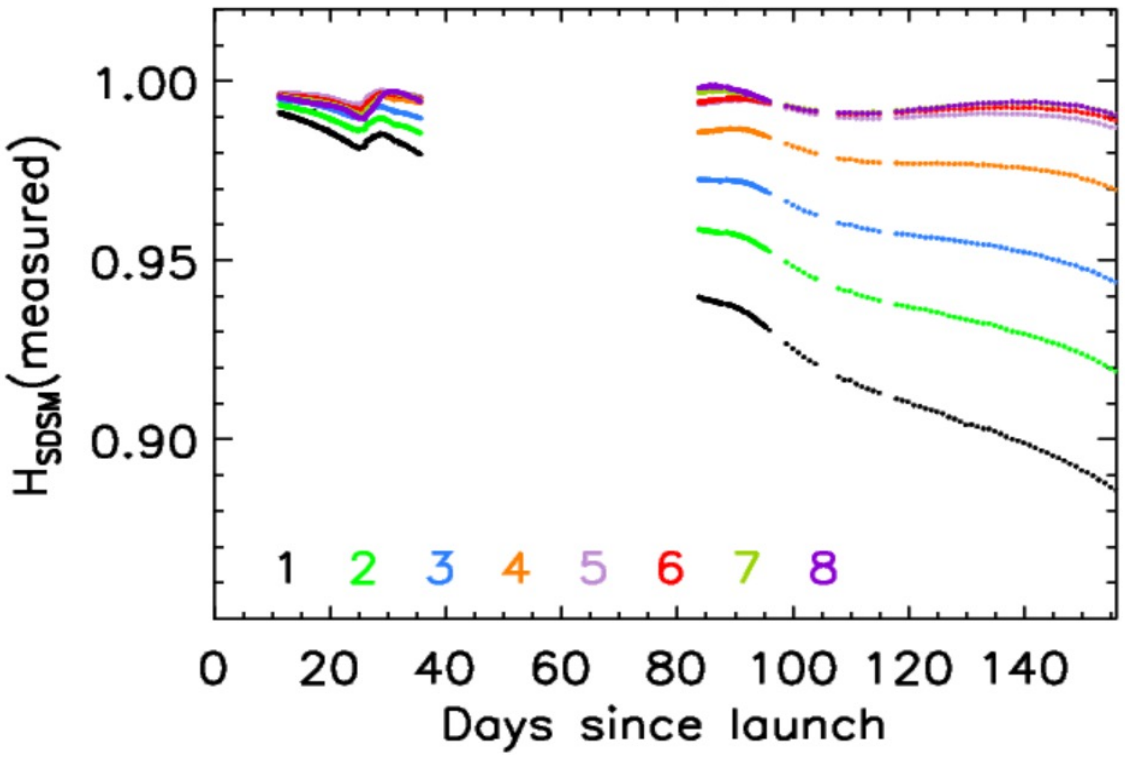

N-21 SDSM Detector Gains

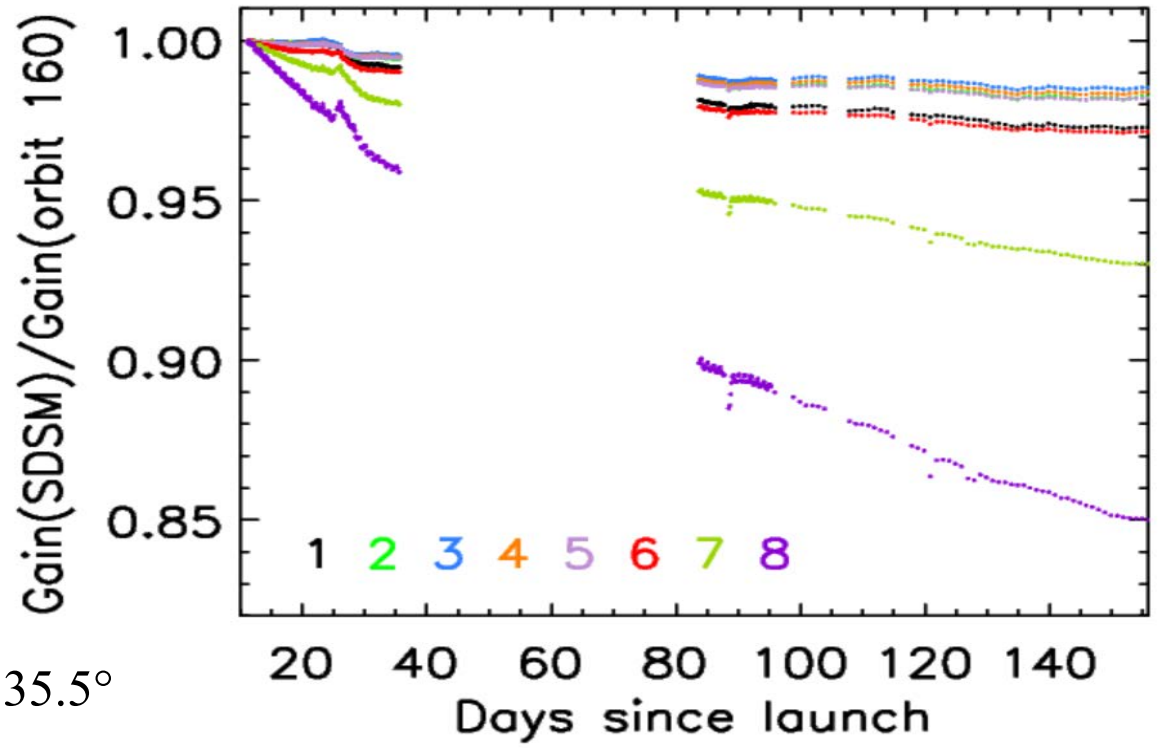

$\phi_V = 35.5°$

- **H-factors decrease faster than N-20 and similarly to S-NPP H-factors**
- **SDSM gains decrease similarly to S-NPP and N-21**
- **Undulation in the H mainly from screen function errors (will be improved later this year)**

Performance of N-21 RSBs: F-factors

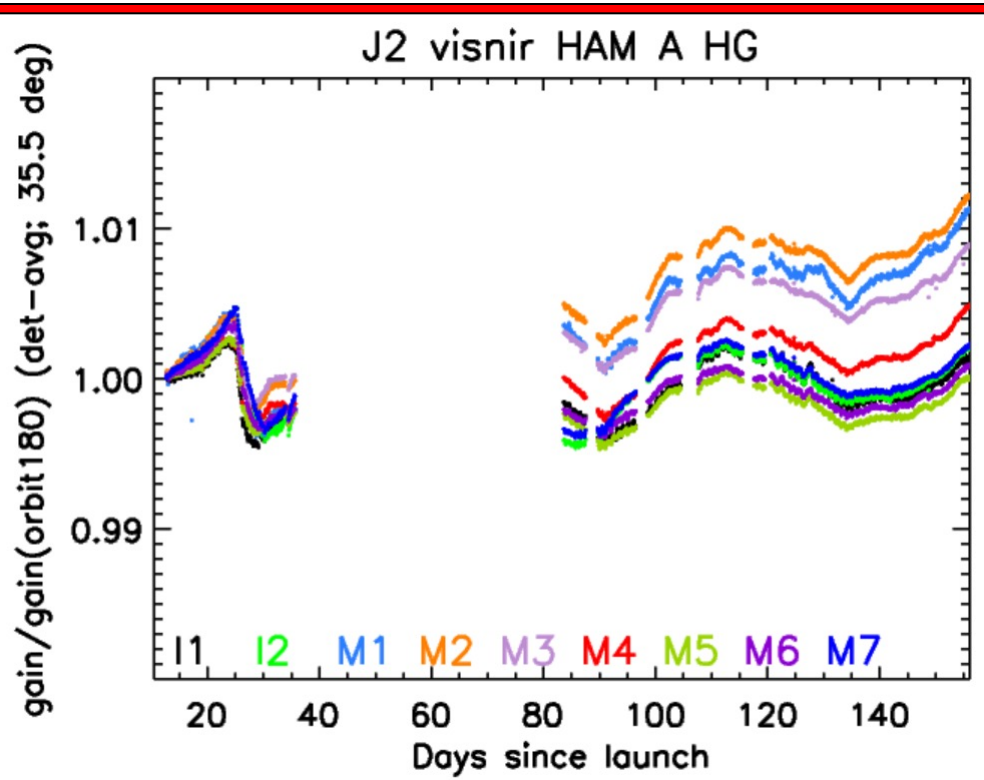

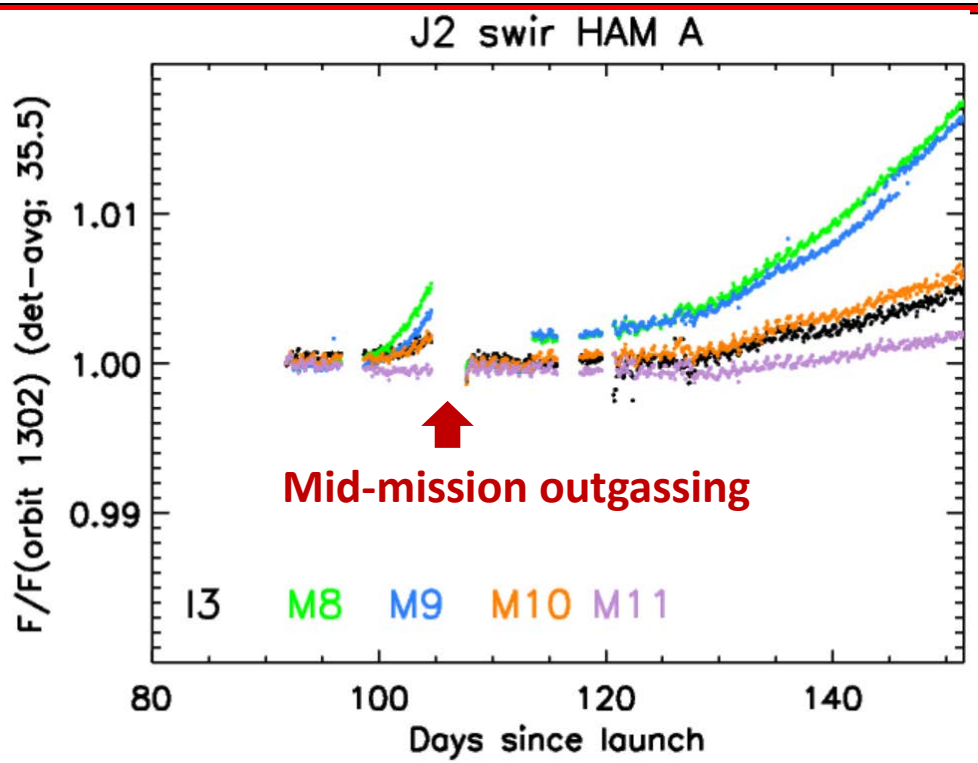

- VISNIR bands: F(SD, with measured H_{SDSM}) has a downward trend
- SWIR bands: F(H=1) trends upwards, likely because of ice accumulation on focal plane

SNRs

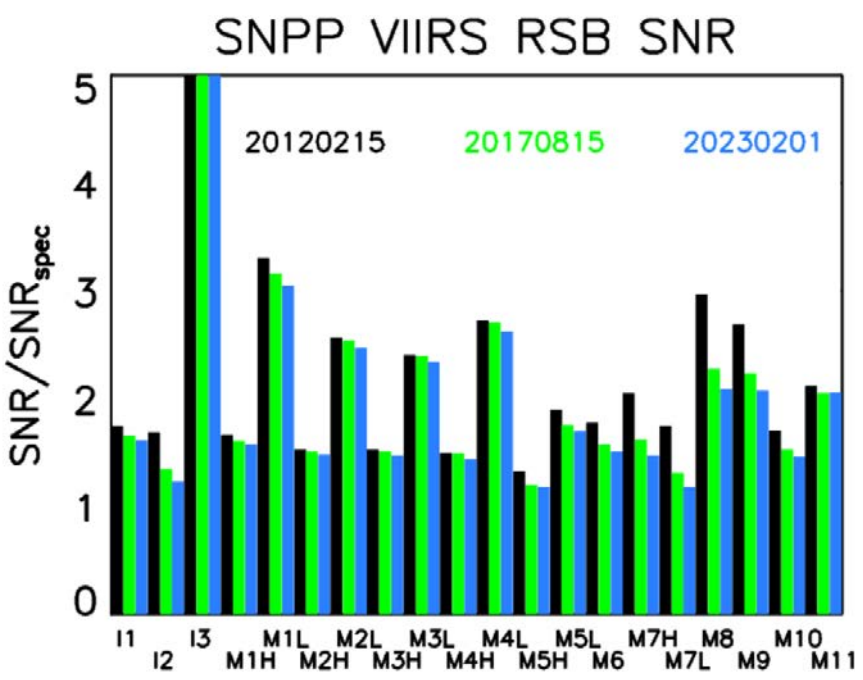

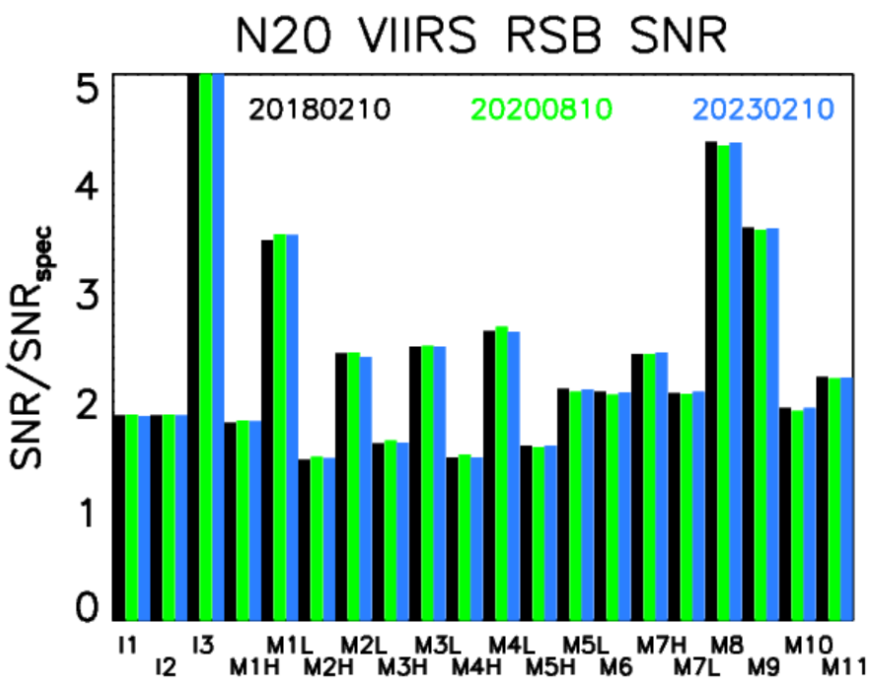

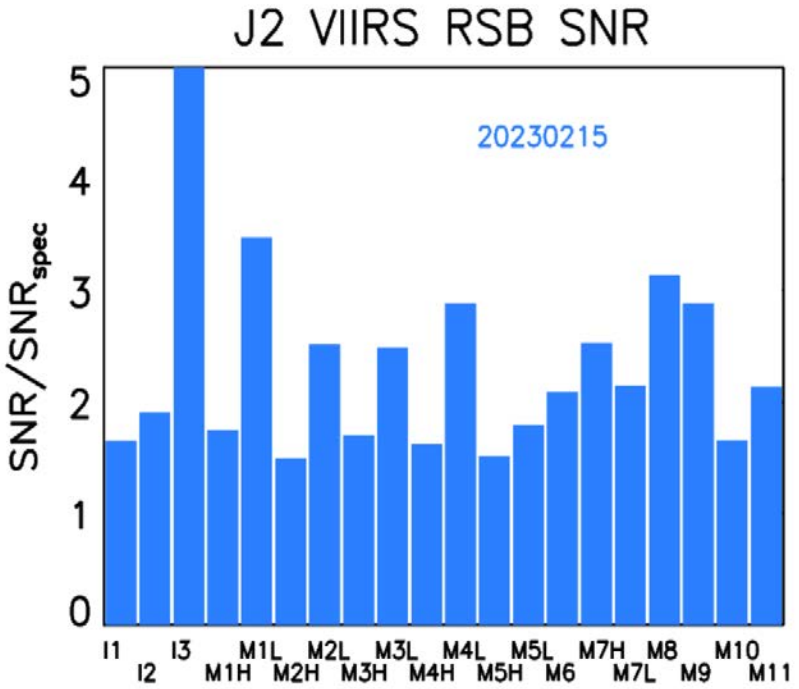

All SNRs satisfy requirements, except N-20 I3 band detector 29 (noisy detector)

S-NPP H-factor SD positional dependence

SD BRDF change factor (H-factor) can depend on SD position

detector array

model parameters

$$H_{\mathrm{RTA}}\left(\lambda, t, \phi_{\mathrm{H,SD}}^{\mathrm{RTA}}, \vec{r}_d\right) =$$

$$H_{\mathrm{RTA}}\left(H_{\mathrm{SDSM}}(\lambda, t), \phi_{\mathrm{H,SD}}^{\mathrm{RTA}}\right) \times \left[1 + c_{d,1}(d - d_{\mathrm{mid}}) + c_{d,2}(d - d_{\mathrm{mid}}) \times \left(\mathbf{1} - \boldsymbol{H}_{\mathbf{SDSM}}(\boldsymbol{\lambda}, \boldsymbol{t})\right)\right]$$

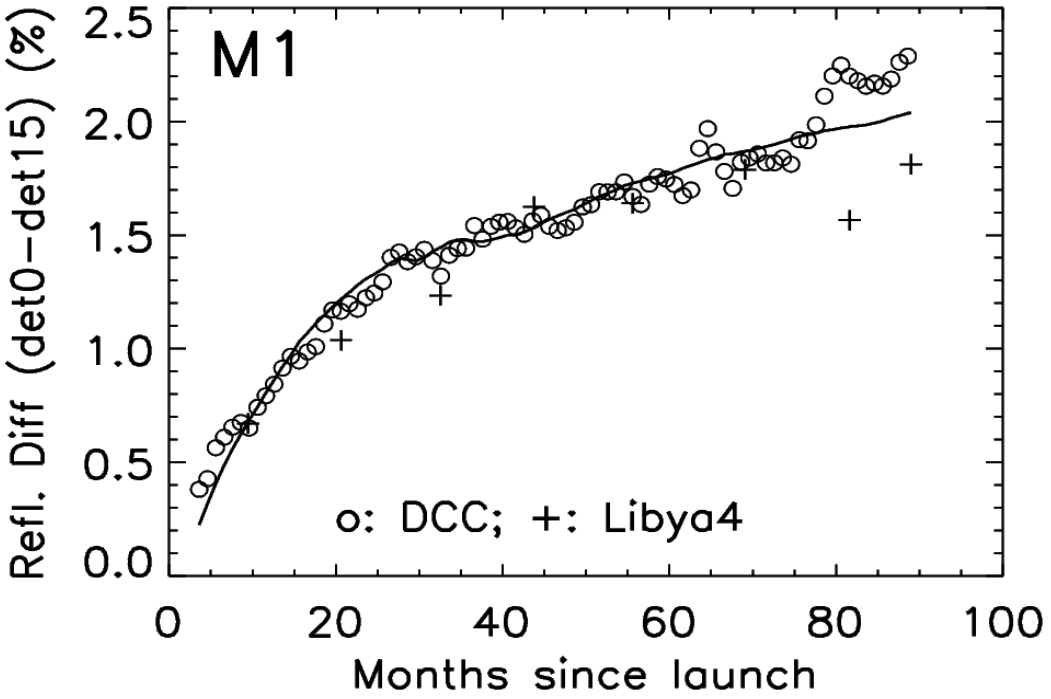

S-NPP TOA images

2019229
M1 striping (C1.1)

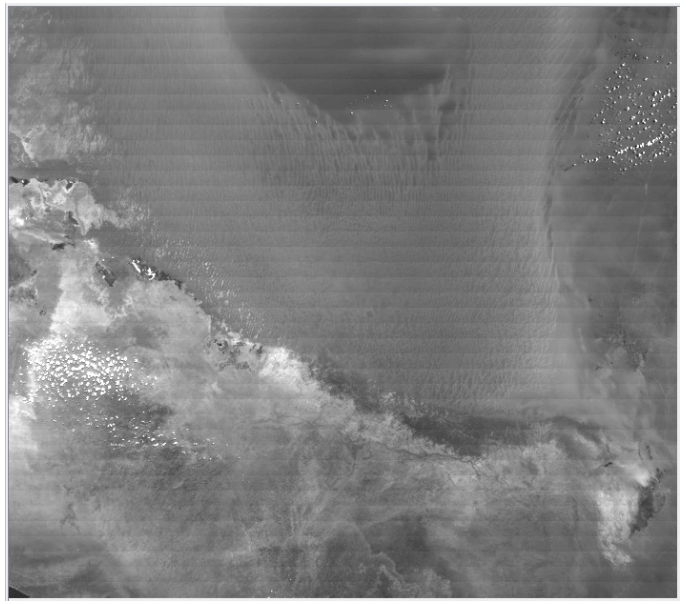

2019229
M1 striping gone (C2.0)

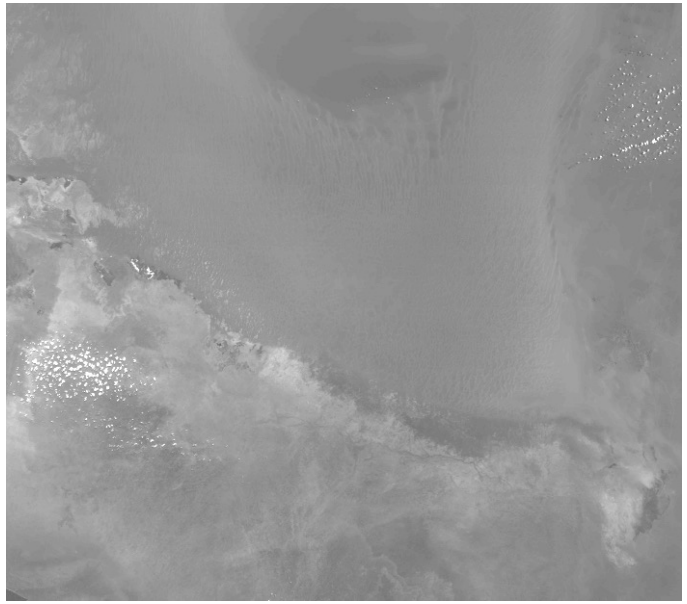

March 2023
No striping seen (C2.0)

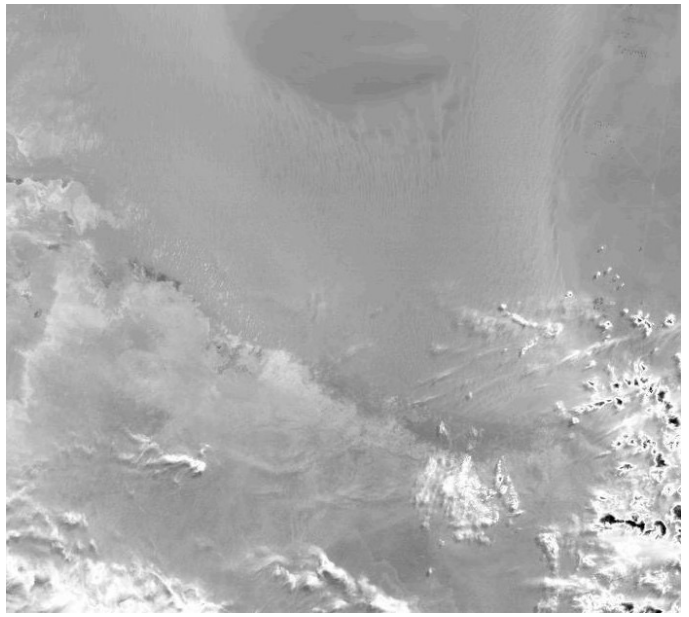

H-factor SD positional dependence algorithm (2017) and results (2018) are still good

Uncertainty of TOA reflectance factor

- **Derive reflectance factor uncertainty from definition**

$$\frac{\mathrm{var}(\rho_{\mathrm{EV}}\cos\theta_{\mathrm{EARTH-SUN}})}{\rho_{\mathrm{EV}}^2(\cos\theta_{\mathrm{EARTH-SUN}})\text{^}2} = \frac{\mathrm{var}(dn_{\mathrm{EV}})}{dn_{\mathrm{EV}}^2} + \frac{\mathrm{var}(H_{\mathrm{RTA}})}{H_{\mathrm{RTA}}^2} + \frac{\mathrm{var}(\tau_{\mathrm{SD}}\mathrm{BRDF}_{\mathrm{RTA}}(t{=}0))}{[\tau_{\mathrm{SD}}\mathrm{BRDF}_{\mathrm{RTA}}(t{=}0)]^2} + \mathrm{var}\left[\frac{\mathrm{RVS}(\theta_{SD})}{\mathrm{RVS}(\theta_{EV})}\right]$$

$$+ var(c_{2,1})(dn_{EV} - dn_{SD})^2 + \frac{\mathrm{var}(\cos(\theta_{\mathrm{SUN-SD}}))}{\cos^2(\theta_{\mathrm{SUN-SD}})}$$

- **Uncertainty LUTs are generated for L1B code for S-NPP and N-20**

Reference: VCST_TECH_REPORT_2022_009

Improvement in detecting saturation/rollover

Original rollover flagging (black dots)

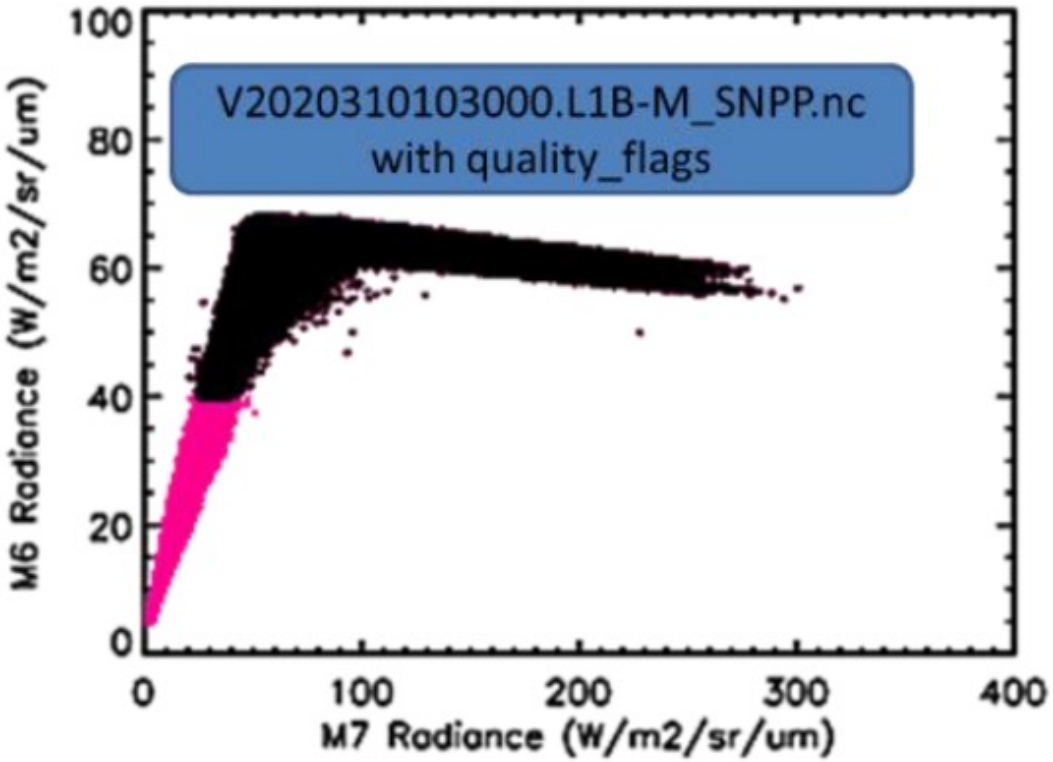

Current rollover flagging (black dots)

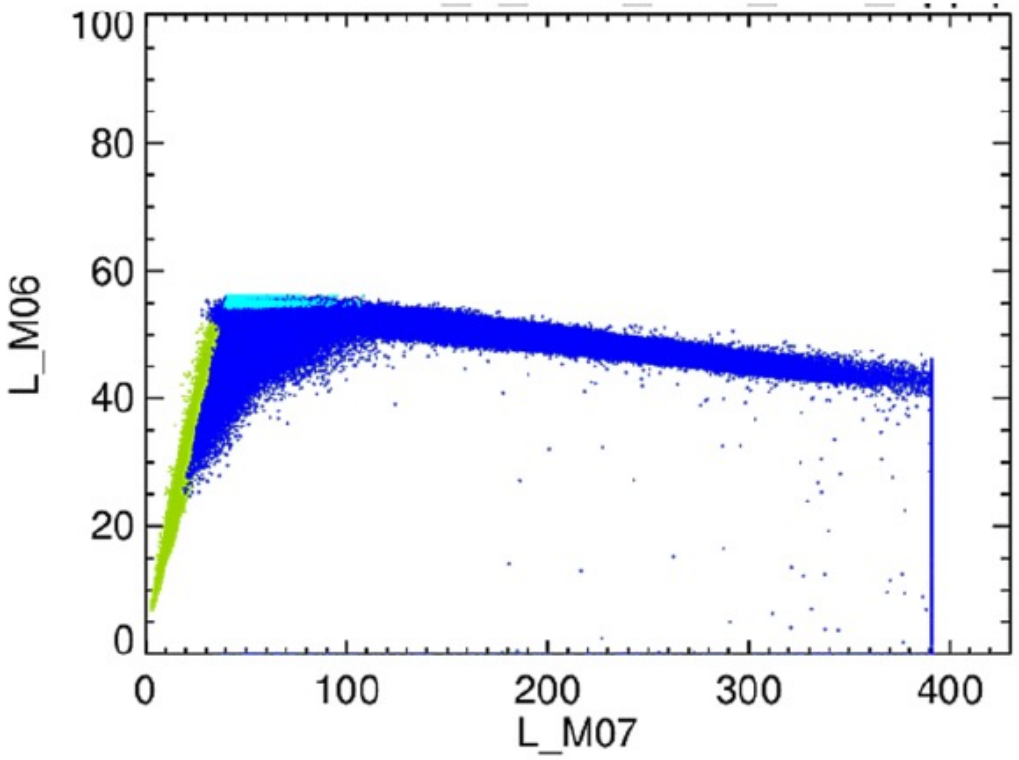

Use neighboring band radiance as a reference, in additional to its own radiance

Reference: A. Angal et al., SPIE Proc. Vol. 12232 (2022)

Future works

1. N-20 RSB striping mitigation

2. Improve N-21 screen functions with data collected at both yaw maneuvers and regular orbits

3. S-NPP M6 saturation flagging

Summary

- S-NPP, N-20, and N-21 VIIRS RSBs perform normally with SNRs satisfying specifications (except N-20 I3 detector 29) and will remain above specifications for the foreseeable future
- Used N-20 RSB F(moon) to find H_{RTA} from H_{SDSM}, instead of using S-NPP H_{RTA} results, a sliding window approach
- Developed L1B reflectance uncertainty algorithm, delivered uncertainty LUTs
- Improved saturation detection algorithm